

Published in final edited form as:

Nat Neurosci. 2015 April ; 18(4): 553–561. doi:10.1038/nn.3957.

Neuronal ensembles sufficient for recovery sleep and the sedative actions of α_2 adrenergic agonists

Zhe Zhang^{#1}, Valentina Ferretti^{#1}, Ike Güntan¹, Alessandro Moro¹, Eleonora A. Steinberg¹, Zhiwen Ye¹, Anna Y. Zecharia¹, Xiao Yu¹, Alexei L. Vyssotski², Stephen G. Brickley¹, Raquel Yustos¹, Zoe E. Pillidge¹, Edward C. Harding¹, William Wisden^{1,*}, and Nicholas P. Franks^{1,*}

¹Department of Life Sciences Imperial College London, South Kensington, SW7 2AZ, U.K.

²Institute of Neuroinformatics, University of Zürich/ETH Zürich, Winterthurerstrasse 190, CH-8057, Zürich, Switzerland

These authors contributed equally to this work.

Abstract

Do sedatives engage natural sleep pathways? It is usually assumed that anesthetic-induced sedation and loss-of-righting-reflex (LORR) arise by influencing the same circuitry to lesser or greater extents. For the α_2 adrenergic receptor agonist dexmedetomidine, we find that sedation and LORR are in fact distinct states, requiring different brain areas, the preoptic hypothalamic area and locus coeruleus (LC) respectively. Selective knockdown of α_2A adrenergic receptors from the LC abolished dexmedetomidine-induced LORR, but not sedation. Instead, we found that dexmedetomidine-induced sedation resembles the deep recovery sleep that follows sleep deprivation. We used TetTag-pharmacogenetics in mice to functionally mark neurons activated in the preoptic hypothalamus during dexmedetomidine-induced sedation or recovery sleep. The neuronal ensembles could then be selectively reactivated. In both cases NREM sleep, with the accompanying drop in body temperature, was recapitulated. Thus α_2 adrenergic receptor-induced sedation and recovery sleep share hypothalamic circuitry sufficient for producing these behavioral states.

Introduction

Sedatives target just a handful of receptors and ion channels^{1,2}. But explaining how activating these receptors produces sedation presents a challenge². In particular, do sedatives

Users may view, print, copy, and download text and data-mine the content in such documents, for the purposes of academic research, subject always to the full Conditions of use:http://www.nature.com/authors/editorial_policies/license.html#terms

*Correspondence should be addressed to: Professor Nick Franks or Professor William Wisden, Department of Life Sciences, Sir Ernst Chain Building, Imperial College London, South Kensington, London SW7 2AZ, UK. Tel: + 44 (0) 20 7594 7629
n.franks@imperial.ac.uk or w.wisden@imperial.ac.uk.

N.P.F. and W.W. conceived and designed the experiments, Z.Z., V.F., I.G., A.M., E.A.S., Z.Y., A.Y.Z., X.Y., R.Y., Z.E.P. and E.C.H. performed the experiments, A.L.V. provided the Neurologgers, N.P.F., W.W. and S.G.B. contributed to the data analysis and N.P.F. and W.W. wrote the paper.

A Supplementary Methods Checklist is available

act at specific brain locations and circuitries or more widely? Some powerful sedatives such as clonidine, guanfacine, xylazine and dexmedetomidine are agonists at inhibitory metabotropic adrenergic α_2 receptors. Amongst these, dexmedetomidine is being assessed as an alternative to benzodiazepines for sedating patients during intensive care³. It induces a state resembling non-rapid-eye-movement (NREM) sleep, with lowered body temperature and enhanced slow wave activity in the neocortex⁴⁻⁶.

At the circuit level it is unclear how α_2 agonists induce sedation and loss of consciousness in humans, or the presumed surrogate, loss of righting reflex (LORR) in animals⁷. The most popular proposal hinges on the selective inhibition, by α_2A (*adra2a*) receptors, of noradrenergic neurons in the locus coeruleus (LC)⁷⁻¹¹. These neurons fire during waking, do so less during sleep, and their activity increases just before waking, suggesting they promote wakefulness¹²⁻¹⁴. Although selectively stimulating LC neurons induces waking¹⁵, the converse is not true: acutely inhibiting LC neurons does not produce strong sleep, even after 1 hour of stimulation¹⁵, an unexpected result if α_2 agonists are supposed to acutely inhibit the LC to induce hypnosis. Moreover, dexmedetomidine still induces LORR in mice unable to synthesize noradrenalin (NA)^{7,16,17}, although without the endogenous ligand, α_2A -receptor responses elsewhere become hypersensitized long-term^{7,17}, making interpretation of this observation difficult⁷.

In this paper, we hypothesize that the heavy, but arousable nature of α_2 agonist-induced sedation might be most similar to the NREM sleep experienced after sleep deprivation, so-called “recovery sleep”. In both cases there is a strong urge to enter deep sleep. One place where these effects might come together is the preoptic (PO) hypothalamus. The PO area, a mixture of sleep-active, wake-active, temperature-sensitive and state-indifferent neurons¹⁸⁻²⁰, houses circuitry which initiates and/or maintains sleep^{18,19,21-23}, and regulates body temperature¹⁸.

We first used siRNA knockdown, which established that although dexmedetomidine-induced LORR depended on activating α_2A receptors on LC neurons, sedation did not, suggesting that these states depend on different neuronal populations. We next explored whether the two types of deep sleep - the sedation imposed by dexmedetomidine and the recovery sleep following sleep deprivation, together with the accompanying drop in body temperature - required similar neural circuitry. For this we combined TetTagging with DREADD pharmacogenetics (TetTag-DREADD)²⁴⁻²⁶. We “tagged” neuronal ensembles in the PO hypothalamus activated during recovery sleep or dexmedetomidine-induced sedation, and then caused these “tagged ensembles” to be selectively reactivated using the hM₃D_q receptor and its ligand clozapine-N-oxide (CNO)²⁷. In both cases reactivating the ensemble for sedation or recovery sleep produced sustained NREM sleep, together with a lower body temperature. We found that recovery sleep and α_2 adrenergic receptor-induced sedation were not only similar behavioral states, but were both induced by activating similar neuronal populations in the PO hypothalamus.

RESULTS

Sedation and LORR require distinct neuronal populations

We examined dexmedetomidine's action at α_2A receptors selectively in the LC, using acute knockdown of *adra2a* transcripts, and determined how this affected sedation and LORR. We first selected two *adra2a* shRNA sequences to use *in vivo*. For this, four putative *adra2a* shRNA sequences (*shadra2a*) were placed into a microRNA gene, *mir30²⁸* (Fig. 1a). Two of the *adra2a* hairpin sequences (*shadra2a₁* & *shadra2a₂*) substantially reduced GFP expression from a reporter gene, *adra2a-IRES-gfp* co-expressed in HEK293 cells; results using one of these, *dsRED-mir30-shadra2a₁*, are shown (Fig. 1a). The *dsRED-mir30-shadra2a₁*, *dsRED-mir30-shadra2a₂* and *dsRED-mir30-shscramble* cassettes were then placed into adeno-associated virus (AAV) genomes, packaged, and injected bilaterally into the LC (Fig. 1b). In the following section, similar results were obtained with both *shadra2a* sequences; all *in vivo* results are illustrated for *shadra2a₁*. The treated animals are termed: LC-*adra2a-KD* and LC-*scramble* respectively. We obtained, on average, a knockdown to $46.3 \pm 9.2\%$ (mean \pm SE) of control *adra2a* transcript levels (*t*-test, $P < 0.004$, compared with mRNA levels in the LC area of LC-*scramble* mice). We prepared acute slices from brainstem of LC-*adra2a-KD* and LC-*scramble* mice and examined the electrophysiological responses of LC noradrenergic neurons to the α_2 agonist dexmedetomidine (Fig. 1c left). Dexmedetomidine (1 μ M), when applied to LC-*scramble* neurons inhibited action potential firing, hyperpolarizing the membrane potential by 9.8 ± 2 mV (mean \pm s.e.m.; $n=6$ cells), as shown previously for other noradrenergic α_2 agonists^{9,10,29}. However, in LC-*adra2a-KD* neurons, dexmedetomidine failed to block action potential firing (Fig. 1c right) and the membrane potential did not change significantly ($P=0.7$; $n=7$ cells). Thus the knockdown of *adra2a* gene expression by approximately 50% removed the ability of dexmedetomidine to silence LC neurons. This is in agreement with studies on heterozygote *adra2a* global knockout mice, which found that the *adra2a* allele shows strong haplo-insufficiency, whereby even at a high dose of dexmedetomidine (433 μ g/kg), dexmedetomidine-induced LORR in *adra2a* knockout mice was abolished³⁰.

We next injected a high dose of dexmedetomidine (400 μ g/kg *i.p.*) into LC-*scramble* or LC-*adra2a-KD* mice. All LC-*scramble* mice ($n=9$) achieved LORR measured 10 minutes after dexmedetomidine injection; there was a concomitant large increase in delta power in the EEG (Fig. 1d, right). By contrast, only 25 % of LC-*adra2a-KD* mice achieved LORR following dexmedetomidine injection ($n=8$, Fisher's exact test, $P=0.0023$); there was still an increase in EEG delta power in these mice, but it was about half that of control (scramble-injected) mice (Fig. 1d, right). Thus, we found that, in contrast to studies in mice with global dopamine- β -hydroxylase knockouts^{16,17}, but in agreement with earlier proposals¹¹, α_2A receptors on LC neurons are needed for α_2 adrenergic agonist-induced LORR, and their knock-down causes a reduction in dexmedetomidine-induced delta power. We next gave a separate group of LC-*adra2a-KD* and LC-*scramble* mice lower doses of dexmedetomidine (12.5–100 μ g/kg). Both groups of mice showed equal ($P=0.91$) sedation (Fig. 1e), becoming immobile and crouched, and with lowered heads. If prodded, they did respond briefly by walking but then stopped. All sedated mice showed increases in EEG delta power ($n=5$) (Fig. 1d, middle), whether or not the α_2A receptor had been knocked down. Thus α_2A

receptor expression on LC neurons was not necessary for α_2 adrenergic receptor-induced sedation, a conclusion that surprised us, given that it was necessary for LORR. We thus reasoned that α_2A agonist-induced LORR and sedation are distinct states, involving different neuronal groups.

TetTagging neurons in the preoptic hypothalamus

If not at the LC, where in the mouse brain is the α_2 receptor-induced sedative response taking place, and could natural sleep pathways be involved? Previous work emphasized that the ventro lateral preoptic (VLPO) nucleus in the PO hypothalamus was activated following dexmedetomidine administration⁸, and during normal and recovery sleep^{21,31}, so we reviewed cFOS activation in the PO area. Mice were injected with a sedative dose of dexmedetomidine (100 $\mu\text{g}/\text{kg}$) or control saline. Brains were taken either 30 or 60 minutes afterwards, and analyzed for endogenous cFOS expression (Fig. 2 and Supplementary Fig. 1). We also investigated cFOS expression 2 hours into the recovery sleep following 4 hours of sleep deprivation (Fig. 2 and Supplementary Fig. 1). Although for both dexmedetomidine-induced sedation and during recovery sleep, there were some cFOS positive neurons in VLPO, many more activated cells were found in the wider PO area (LPO, MPO) and in a cluster of areas just dorsal of the preoptic region, in the BST (*e.g.* in the STMA and STLD), and in several septal nuclei: the ventral lateral septum (LSV) and in the septo-hypothalamic nucleus (SHy) (Fig. 2a,b,c). Thus, the broadly similar patterns of induced cFOS during dexmedetomidine-induced sedation and during recovery sleep, indicated that much of the PO region was a suitable location for TetTag-DREADD mapping²⁴⁻²⁷ to see if activating neurons in this location was sufficient for these behavioral states. We aimed to express, by TetTagging²⁴, a *cfos*-promoter-inducible *hM₃D_q-mCHERRY* receptor gene^{25,27} selectively in the PO area of the hypothalamus. The excitatory *hM₃D_q* metabotropic receptor is uniquely activated by the ligand CNO²⁷. By combining this receptor with *cfos*-dependent TetTagging, the gene encoding the *hM₃D_q* receptor is only turned on following neural activity, and so records, or “tags” ensembles of neurons that have been activated *in vivo* by a stimulus²⁵. The neurons can then be reactivated later by systemic CNO, allowing sufficiency for the particular behavior²⁵, sleep in this case, to be tested.

TetTagging has been developed with transgenic mice^{24,25}. We set up the system using AAV genomes so that we could target the PO hypothalamus. Because of size constraints of the AAV genome, we generated two AAV viruses, one which contained the *P_{cfos}-tTA* transgene, and the other which contained the *tet-operator* promoter (*P_{TRE-tight}*) linked to an *hM₃D_q-mCHERRY* receptor reading frame (Fig. 3a). With this method, before the behavioral experiments are undertaken, the TetTag system is repressed with doxycycline in the diet. Doxycycline prevents tTA activating its target promoter, *P_{TRE-tight}*, located in the second AAV genome; when doxycycline is removed, neural activity, *e.g.* taking place in recovery sleep or dexmedetomidine-induced sedation, can drive the *cfos* promoter-linked tTA expression, which in turn can activate *hM₃D_q-mCHERRY* expression (Fig. 3a).

Preliminary experiments showed that when AAV-*P_{cfos}-tTA* and AAV-*P_{TRE-tight}-hM₃D_q-mCHERRY* were co-injected, neurons were co-transduced. We therefore co-injected both the AAV-*P_{cfos}-tTA* and AAV-*P_{TRE-tight}-hM₃D_q-mCHERRY* bilaterally into LPO (“LPO-

TetTag-hM₃D_q” mice) or centrally into the median PO, MnPO, (“MnPO-*TetTag-hM₃D_q*” mice), the latter being an area where neurons are particularly active in recovery sleep following sleep deprivation¹⁹. The subsequent experimental schemes are outlined in Fig. 3b. We maintained the mice for 4 weeks on a doxycycline diet. Doxycycline was then removed from the diet to allow potential inducibility of the *hM₃D_q-mCHERRY* gene, and 2 days later mice were given either a sedative dose of dexmedetomidine (100 µg/kg) *i.p.* or a control saline injection *i.p.* or four hours of sleep deprivation, and then allowed recovery sleep. In about half of the cohort, the dexmedetomidine injection and sleep deprivation procedures were switched (Fig. 3b). The order of these procedures made no difference to the results. We did several controls for the specificity of the TetTag-DREADD system (see Supplementary text).

In the virally injected animals, we looked at activity inducible *hM₃D_q-mCHERRY* patterns in the LPO and MnPO. We looked at TetTag gene expression in these areas before and after mice were given the sedative dose of dexmedetomidine (100 µg/kg) or sleep deprived and then killed during recovery sleep (Fig. 3c and Supplementary Fig. 2). LPO-*TetTag-hM₃D_q* and MnPO-*TetTag-hM₃D_q* brains were taken 2 hours before, or 2 hours after animals received dexmedetomidine or a control saline injection, or 2 hours into recovery sleep. They were analyzed for *mCHERRY* expression. Before dexmedetomidine injection or sleep deprivation, but with no doxycycline present, there was a low but detectable level of *P_{TRE-tight}-hM₃D_q-mCHERRY* transgene expression in scattered cells throughout the injected area in both the LPO-*TetTag-hM₃D_q* mice or the MnPO-*TetTag-hM₃D_q* mice (Fig. 3c and Supplementary Fig. 2). This basal transgene expression was also present with doxycycline. In LPO-*TetTag-hM₃D_q* brains, and in agreement with the induction of the endogenous *cfos* gene (Fig. 2), a wide area expressed *hM₃D_q-mCHERRY* receptors following systemic dexmedetomidine administration, stretching from the bed nucleus stria terminalis/lateral septum and septal hypothalamic nuclei in the dorsal part of the region, the whole LPO area and through to the VLPO and extended VLPO area at the base (Fig. 3c). For recovery sleep, a similar LPO-*P_{TRE-tight}-hM₃D_q-mCHERRY* transgene expression pattern was found; this expression started to already appear during the sleep deprivation period, and had become stronger two hours into recovery sleep (Fig. 3c). For the MnPO-*TetTag-hM₃D_q* brains, recovery sleep and dexmedetomidine-induced sedation both induced *hM₃D_q-mCHERRY* transgene expression above basal levels in the MnPO area; however, there was a differential effect, because the gene induction was weaker following dexmedetomidine-induced sedation compared with that during recovery sleep (Supplementary Fig. 2). In separate experiments we determined that levels of the induced *hM₃D_q-mCHERRY* receptor protein persisted for at least 4 days post-stimulus (*e.g.* dexmedetomidine-induced sedation or recovery sleep after sleep deprivation followed immediately by doxycycline in the diet – Fig. 3c and Supplementary Fig. 2), but that during the 4-week period following the first challenge, sleep-deprivation or dexmedetomidine-induced sedation, levels *TetTag-hM₃D_q-mCHERRY* transgene expression had fallen back to baseline levels (Fig. 3c and Supplementary Fig. 2). The range of induced transgene expression patterns is summarized in Supplementary Figs. 3 and 4.

CNO induced the expression of *cfos* protein in TetTagged *hM₃D_q-mCHERRY*-positive neurons (Supplementary Fig. 5), suggesting that an excitatory response was generated in

these neurons. To confirm this, we patch-clamped visually identified (*mCHERRY*-positive) Tet-Tagged neurons found in acute PO slices after dexmedetomidine-induced sedation. In neurons that were TetTagged, we found that CNO induced an excitatory response (8 out of 8 neurons in 3 animals), and could trigger action potential firing (Supplementary Fig. 6a). The average depolarization was 10.2 ± 2.1 mV in response to 5 μ M CNO. As expected, these results are consistent with the hM_3D_q receptor coupling to excitatory mechanisms²⁷. After recording from the TetTagged neurons, we used single-cell qPCR to determine their type: 84% were GABAergic (*gad1* and/or *gad2* expression); the remaining were glutamatergic (*vglut2* expression) (Supplementary Fig. 6b,c).

Recapitulation of recovery sleep and sedation by CNO

The following sequence of results is illustrated with LPO-*TetTag-hM₃D_q* and MnPO-*TetTag-hM₃D_q* mice first undergoing dexmedetomidine-induced sedation, followed by CNO treatment, then after a one month gap, 4 hours sleep deprivation and recovery sleep followed by CNO treatment (Figs. 4 and 5). Approximately five minutes after dexmedetomidine injection, the EEG of both LPO-*TetTag-hM₃D_q* and MnPO-*TetTag-hM₃D_q* mice exhibited prominent and sustained NREM which lasted ~90 minutes relative to the mice given only saline (Figs. 4a and 5a). All dexmedetomidine-injected mice became immobile (Fig. 4b), but still had a righting reflex. Mice were then put back on the doxycycline diet for 4 days to repress the induction of further *TetTag-hM₃D_q* receptors, and after this injected *i.p.* with CNO or saline and their EEG and behavioral responses recorded (Figs. 4c,d and 5b). (The mice used in our study exhibited maximal periods of NREM sleep during the “lights on” part of the cycle (Supplementary Fig. 7a,b). All CNO injections were therefore carried out during this period when the mice were most active.)

After CNO injection, the LPO-*TetTag-hM₃D_q* mice went into a state resembling sustained NREM sleep (Figs. 4c,d and 5b). They moved little, and their neocortical EEG developed powerful and sustained delta activity for about 90 minutes. Thus dexmedetomidine-induced sedation was recapitulated by CNO injection.

Giving CNO to the MnPO-*TetTag-hM₃D_q* mice that were previously sedated with dexmedetomidine induced significant delta power (high delta/theta ratio) in the EEG (Figs. 4c and 5c), but these mice kept moving to a similar extent to the saline or CNO injected controls (Fig. 4d). Thus there was a notable disconnect between EEG and behavior. This suggests that the LPO area, but not the MnPO, contains neurons sufficient for full adrenergic α_2 receptor-induced sedation.

Prior to the next stimulus, sleep deprivation followed by recovery sleep, LPO-*TetTag-hM₃D_q* and MnPO-*TetTag-hM₃D_q* mice were maintained on doxycycline for a further 4 weeks. CNO administration to these animals during the latter part of this time had no effect on the behavior or EEG, consistent with the decay of the *hM₃D_q-mCHERRY* protein back to basal levels (See Fig. 3c and Supplementary Fig. 2). About a month after the first experiment (dexmedetomidine-induced sedation), the mice were removed from doxycycline, and 48 hours later, instead of a sedative dexmedetomidine injection, the mice were sleep deprived and then allowed a period of recovery sleep (Fig. 4e). During the recovery sleep, the EEG of both LPO-*TetTag-hM₃D_q* and MnPO-*TetTag-hM₃D_q* mice showed sustained NREM sleep

(Figs. 4e and 5d). During a 30-minute recording, mice in recovery sleep moved little (Fig. 4f). After the period of sleep deprivation the mice were placed back on doxycycline, and four days later given a CNO or saline injection *i.p.* and their behavior and EEG responses measured.

Both groups of CNO-injected mice, LPO-*TetTag-hM₃D_q* and MnPO-*TetTag-hM₃D_q* mice, had sustained delta power ~90 minutes following CNO administration (Figs. 4g and 5e,f), and strong behavioral arrest (Fig. 4h), showing that an ensemble of neurons had been activated in these areas that were sufficient to initiate and sustain recovery sleep. Given that these were the same group of animals that had earlier undergone dexmedetomidine-induced sedation and reactivation by CNO, it seems likely that dexmedetomidine-induced sedation and recovery sleep share similar mechanisms and circuitry for the LPO area. On the other hand, although MnPO seemed relevant for recovery sleep, where its re-activation seemed to be as effective as LPO's, MnPO played less of a role in dexmedetomidine-induced sedation.

Recapitulation of hypothermia by CNO

Using TetTagging, we examined if the neural circuitries in the LPO and MnPO areas were sufficient to trigger sedative or recovery sleep-induced hypothermia. Before any treatments, we checked that neither saline or CNO injections caused a change in body temperature (Fig. 6a). The body temperature of the mice was higher during the dark period when they were most active (Supplementary Fig. 7c); as for the sedation experiments, all investigations of temperature were done during the dark period. Two days after doxycycline removal, the LPO-*TetTag-hM₃D_q* and MnPO-*TetTag-hM₃D_q* mice were given the sedative dose of 100 µg/kg dexmedetomidine. This caused a strong hypothermia (Fig. 6a), consistent with previous reports^{6,32}. Four days later, on a doxycycline diet, they were then injected with CNO. In the LPO-*TetTag-hM₃D_q* animals, CNO reactivation of the dexmedetomidine-induced hypothalamic ensembles largely recapitulated the temperature drop (Fig. 6b). There was, however, little effect in MnPO-*TetTag-hM₃D_q* mice (Fig. 6c). Thus following dexmedetomidine sedation, activated neuronal ensembles in LPO, but not MnPO, are responsible for the hypothermia produced by this drug.

A parallel group of LPO-*TetTag-hM₃D_q* and MnPO-*TetTag-hM₃D_q* mice were sleep deprived for four hours and allowed recovery sleep. Sleep deprivation elevated their body temperature to about 38°C; during the first few hours of recovery sleep this temperature fell to that occurring during natural NREM sleep, about 36.5°C (Fig. 6d and Supplementary Fig. 7c). Four days later, mice were given CNO. In both the LPO- and MnPO-*TetTag-hM₃D_q* groups, CNO treatment produced a substantial drop in body temperature (Fig. 6e,f), comparable to, but somewhat larger than that seen during recovery sleep (Fig. 6d). Thus, as we found for the effects on delta power and immobility, both LPO and MnPO can contribute equal and parallel effects in producing hypothermia in recovery sleep.

Role of GABAergic neurons for the rapid onset of sedation

To test if dexmedetomidine-induced sedation required GABAergic neurons in the LPO area, we deleted the vesicular GABA transporter (*vgat*) gene by injecting AAV-*Cre-2A-Venus* bilaterally into the LPO of mice homozygous for a floxed *vgat* gene³³, *vgat*^{lox/lox}, to give

LPO- *vgat* mice (Fig. 7a). Control *vgat*^{lox/lox} mice were injected with AAV-*GFP* to give LPO-*GFP* mice.

One month later, when given sedative doses of dexmedetomidine (100 µg/kg), and some five minutes after injection, control LPO-*GFP* mice showed the expected large increase in delta power in their EEG compared with that produced by saline injection (Fig. 7b), they had sustained NREM lasting for ~90 minutes (Fig. 7c), and within about 10 minutes after injection they had ceased moving (Fig. 7d). By contrast, 10 minutes after *i.p.* injection of dexmedetomidine into LPO- *vgat* mice, there was only a small shift of the EEG to delta frequencies (Fig. 7e). This absence of effect was striking (compare Fig. 7b and Fig. 7e). However, ~30 minutes after injection, the percentage of NREM in the LPO- *vgat* mice was significantly higher than saline injected animals (Fig. 7f), and the mice became sedated (Fig. 7g), such that after 30 minutes they were as sedated as dexmedetomidine-injected LPO-*GFP* mice (Fig. 7c,f). Thus GABAergic neurons in the LPO area were required for rapid-onset dexmedetomidine-induced sedation.

DISCUSSION

Selectively activating α 2-adrenoreceptors is an effective way to induce deep but arousable sedation^{7,9,10,34}. The sleep-like qualities of this sedation hint that by understanding how adrenergic α 2 agonists work at the network level, we might learn more about circuitry regulating aspects of natural sleep. Global gene knockouts show that dexmedetomidine-induced sedation, hypothermia and LORR all depend on α 2A receptors^{9,32}. As α 2A receptor activation inhibits noradrenergic LC neurons⁹ (see also Fig. 1c), and LC firing promotes wakefulness¹³⁻¹⁵, the view has been that α 2-adrenergic agonists produce sedation by inhibiting the LC⁷. In many studies, sedation and LORR tend to be conceptually blended: sedation is considered a light or intermittent loss of consciousness, whereas LORR is a deeper version of this same state. We investigated this by acute knockdown of α 2A receptors selectively from the LC. Surprisingly, this did not alter dexmedetomidine's ability to induce sedation at low doses (<100 µg/kg), but did, on the other hand, abolish LORR at high concentrations (400 µg/kg). This suggests that these states, sedation and LORR, are generated by α 2 agonist drugs influencing distinct circuitries; in particular, sedation induced by low-dose dexmedetomidine does not depend on inhibiting the LC.

We suggest that dexmedetomidine-induced LORR is not, in fact, the animal equivalent of deep loss of consciousness in humans, as usually assumed, but instead results from engaging the spinal cord mechanism that produces muscle atonia in REM sleep and cataplexy³⁵. During wakefulness, GABAergic/glycinergic interneurons in the spinal cord and brainstem are inhibited by descending LC inputs³⁵; this descending inhibition is released during REM sleep to give muscle atonia³⁵. Thus over-stimulating the noradrenergic LC neurons optogenetically, probably silencing them by vesicle depletion, caused a cataplexy-like state with muscle atonia¹⁵. Similarly, we speculate that high-dose dexmedetomidine causes LORR by inhibiting LC neurons, which in turn releases interneuron inhibition of motor neurons.

Dexmedetomidine sedation and recovery sleep are similar

In humans, the clinical use for dexmedetomidine is at the lower sedative doses. Thus it is particularly important to understand the mechanism of this sedative component. A classic body of work shows that the PO hypothalamic area regulates wakefulness, sleep and body temperature^{18,23,36,37}. Sleep-active and temperature-sensitive neurons are widespread in the PO area¹⁸⁻²⁰. Indeed, we found that an extensive part of the PO hypothalamus and some neighboring dorsal structures express both endogenous cFOS and the *cfos*-dependent *hM₃D_q-mCHERRY* transgene during recovery sleep and after dexmedetomidine-induced sedation. It was not clear, however, if activating any of these neurons is sufficient to induce sleep or the accompanying decrease in body temperature found with these states. To test their sufficiency, we reactivated the induced TetTag ensembles with systemic CNO.

By artificially reactivating the neurons initially activated by a systemic low-dose of dexmedetomidine, we found that such LPO neurons are sufficient to induce both sedation (NREM sleep) and the accompanying strong hypothermia. The rapid induction of this sedation required GABAergic neurons in the LPO area, but full sedation could still emerge later when GABA release was blocked, implying additional mechanisms. Because some of these neurons release galanin³⁸, this neuropeptide may also play a role. We also found that reactivating the same or similar groups of neurons in the LPO also mimicked recovery sleep and the drop in body temperature after sleep deprivation. Thus TetTagging revealed that dexmedetomidine-induced sedation and recovery sleep are similar states, both requiring activation of neuronal ensembles in the LPO area. In future it will be interesting to disentangle the effects of sleep onset and body temperature decrease. Dexmedetomidine and sleep deprivation also induced TetTag-*hM₃D_q* expression in another PO nucleus, MnPO. Although reactivation of MnPO with CNO did fully recapitulate recovery sleep, it only partially recapitulated DEX-induced sedation. There was an interesting disconnect between a strong increase in the EEG delta/theta ratio, and animal movement – the mice were not sleeping – but perhaps “sleep walking”. This was also true with the hypothermia effects: whereas MnPO could recapitulate the temperature decrease seen in recovery sleep, no ensembles that regulate temperature were activated in MnPO by dexmedetomidine sedation.

The natural sleep rhythm over 24 hours was not a sufficiently strong stimulus to induce the “TetTag-DREADD neuronal ensembles”, at least under our experimental protocol: their formation apparently required the stronger drivers of dexmedetomidine or recovery sleep following sleep deprivation. In basal conditions CNO did not induce a change in the EEG compared with dexmedetomidine sedation and recovery sleep, and animals did not behaviorally enter sleep. Indeed, in mice with *hM₃D_q* receptors selectively but continuously expressed in GABAergic neurons in the PO hypothalamic area³⁹, systemic CNO produced only a small increase in NREM sleep, and only during the day, but not the night.

A dominant hypothesis has been that during wakefulness NA tonically inhibits sleep-active GABAergic neurons in the PO area that project to arousal nuclei^{40,41}. However, the TetTag method demonstrated that both $\alpha 2$ agonists and sleep deprivation induce NREM sleep and decreases in body temperature by locally exciting neurons in the preoptic area. One explanation for our results could be that adrenergic $\alpha 2$ agonists preferentially inhibit local GABAergic interneurons. These, in turn, would then inhibit sleep-active GABAergic

projection neurons less. Thus, following dexmedetomidine administration, the projection neurons would then fire more by dis-inhibition to induce sedation. However, a knockdown of *adra2a* transcripts in the LPO did not alter the sedative effects of 100 μ M dexmedetomidine (Supplementary Fig. 9). Alternatively dexmedetomidine could activate inhibitory α 2A receptors on the terminals of inhibitory afferents coming into the PO area, for example GABA inputs, or NA inputs from nuclei other than the LC. The reduced local release of GABA or NA into the PO hypothalamus would then allow dis-inhibition and excitation of the sleep-promoting neurons.

The biochemical mechanism for how recovery sleep is initiated and maintained remains a mystery. Candidate sleep homeostat molecules, which accumulate proportionally to the amount of sleep deprivation, and act locally in the preoptic area, include PGD2 and adenosine⁴². Because hypothalamic-initiated recovery sleep and dexmedetomidine-induced sedation seem similar, another endogenous, but as yet unidentified, candidate sleep homeostat molecule might resemble an adrenergic α 2 agonist in its properties.

ONLINE METHODS

Design and testing of *adra2a* shRNAs

The mouse *adra2a* coding region, including the start and stop codons, was obtained by PCR from the single exon *adra2* gene in genomic DNA (primer sequences given in reference⁴³) and cloned into an expression plasmid p*P_{cmv}-IRES-gfp* (Clontech) upstream of the *IRES* element, between *XhoI* and *EcoRI* sites, to give p*cmv-adra2a-IRES-gfp* (Fig. 1a). We used the Invitrogen and pSM2 design (http://cancan.cshl.edu/RNAi_central/) algorithms to select shRNAs directed against the mouse *adra2a* coding or 3' UTR regions. To express the shRNAs, we used the pPRIME system²⁸. This generates micro-RNA-30 (mir30)-derived shRNAs and co-expression of a marker protein, such as dsRED, from the same transcript. The shRNA hairpin sequences were placed into the mir30 site of p*PRIME-cmv-dsRed-FF3*²⁸ (Addgene Plasmid 11664; gift from Stephen Elledge). The DNA sequences of the hairpins (21 nucleotides) were:

shadra2a1: 5' -

TGCTGTTGACAGTGAGCGAGCAACGTGCTGGTTATTATCGTAGTGAAGCCACAG

ATGTACGATAATAACCAGCACGTTGCCCTACTGCCTCGGA-3'; *shadra2a2*: 5' -

TGCTGTTGACAGTGAGCGCGCCACTCATCTCCATAGAGAA TAGTGAAGCCACAGA

TGTATTCTCTATGGAGATGAGTGGCGTGCCTACTGCCTCGGA-3'; and *shscramble*:

5' -

TGCTGTTGACAGTGAGCGAGCCGCGATTAGGCTGTTATAATAGTGAAGCCACAGA

TGTATTATAACAGCCTAATCGCGCGGCTTGCCTACTGCCTCGGA-3'.

The hairpin oligonucleotides were PCR amplified by VENT polymerase (NEB, UK) using the pPRIME forward and reverse oligonucleotides with added *XhoI* and *EcoRI* sites underlined (forward: 5' -GATGGCTG-CTCGAG-AAGGTATAT-TGCTGTTGACAGTGAGCG-3'; reverse, 5' -GTCTAGAG-GAATTC-CGAGGCAGTAGGCA-3'), digested with *XhoI* and *EcoRI*, and inserted into the mir30 site of *EcoRI/XhoI*-digested pPRIME to generate the constructs shown in Fig. 1a. To test

knockdown efficiency of the *shadra2* hairpins, HEK293 cells European Collection of Cell Cultures (Salisbury, United Kingdom) were co-transfected, using the calcium phosphate method, with *pP_{cmv}-adra2a-IRES-gfp* and the *pPRIME-dsRED-mir30* plasmids. Sixteen hours after transfection, cells were washed with PBS, and 48 hours afterwards, the coverslips were then fixed, and mounted.

Generation of AAV *shadra2a1*, *shadra2a2* KD and shscramble transgenes

To generate AAV transgene-expressing miRNAs, the *dsRED-mir30-shadra2a1*, *dsRED-mir30-shadra2a2*, and *dsRED-mir30-shscramble* inserts in pPRIME²⁸ were released by *SbfI* and *PacI* digestion, and cloned into the *PstI* and *PacI* sites in the polylinker of the AAV-genome plasmid *pAM-flex*⁴⁴, where we had first changed the *EcoRV* site in the *pAM-flex* polylinker to *PacI*, to give ITR-*cmv P_{enhancer/chicken} β-actin*-dsRED-mir30-shRNA-*woodchuck post-translational regulatory sequence (WPRE)*-*bovine growth hormone polyadenylation signal (pA)*-ITR. These constructs were packed into AAV capsids (see section “Generation of recombinant AAV particles”).

Generation of AAV TetTag-DREADD transgenes

The TetTag transgene components, *cfos-tTA* and *P_{TRE-tight}-hM₃D_q-mCHERRY*, were placed into two separate AAV transgenes. As a building block, we started with the plasmid *pAAV-ITR-P_{cmv/β-actin}-iCre-2A-Venus-WPRE-pA-ITR*⁴⁵. A *PacI* site was first introduced just upstream of the CMV/β-actin promoter in this plasmid using Quick Change Mutagenesis (Agilent) (Primers 5′-CTGGAAGCTCCTTAATTAACGCTCTCCTGTTCCGACC-3′ and 5′-GGTCGGAACAGGAGAGCGTTAATTAAGGAGCTTCCAG-3′), and the “P_{cmv/β-actin}-iCre-2A-Venus” fragment then removed with *PacI* and *NotI* digestion. To generate the AAV-*cfos-tTA* construct, the *cfos-tTA* cassette, from a plasmid containing a *cfos* promoter/first intron -764/+918 fragment (*P_{cfos}*) linked to the tTA reading frame²⁴ (Addgene plasmid 34856; gift from Mark Mayford), was PCR-amplified (the forward primer with a *NotI* site: 5′-GCATTCCACCACTGCGGCCGCTCATCAGTTCCATAGG-3′ and reverse primer with a *PacI* site: 5′-GGTGCGGGCTCTTCTTCTTAATTAAGCCAGACGGCCGACG-3′) and subcloned into the *PacI/NotI* digested Cre-Venus vector, to give *pAAV-ITR-P_{cfos}-tTA-WPRE-pA-ITR*; For the generation of the *pAAV-ITR-P_{TRE-tight}-hM₃D_q-mCherry-WPRE-pA-ITR* construct, we started with the plasmid *pAAV-hSyn-double floxed hM₃D_q-mCHERRY*⁴⁶ (a gift from Bryan L. Roth; Addgene plasmid 44361), which contains an inverted *hM₃D_q-mCherry* reading frame flanked by *AscI* and *NheI* sites. We PCR-amplified (forward primer hM₃D_q-NheI-F: 5′-CGAAGGTTATGGCTAGCCTTACTTGTACAGCTCG-3′; reverse primer hM₃D_q-AscI-R: 5′-CTTTATACGAAGTTATGGCGCGCCACCATGAC-3′) the *hM₃D_q-mCHERRY* reading frame (including the Kozak ATG initiation sequence CCATGG), and placed this fragment back in the *NheI/AcsI* digested parent plasmid, but now in the sense orientation between the *lox* sites to give “*hSyn-double floxed hM₃D_q-mCherry sense*”. We then removed the *hSyn* promoter from this construct by *MluI* and *SalI* digestion, and replaced the promoter with the *TRE-tight (P_{TRE-tight})* promoter; this was PCR-amplified from the *pTRE-Tight* plasmid (Clontech; forward primer, 5′-CTTCACACGCGTTTACTCCCTATCAGGATAGAG-3′; reverse primer, 5′-

CAGCTGACTAGTCGACCCCCGGGTAC-3'), then digested with *MluI* and *SalI*. The final construct was pAAV-*ITR*-*P_{TRE-tight}*-*hM₃D_q*-*mCHERRY*-*WPRE*-*pA*-*ITR*.

Generation of recombinant AAV particles

All AAV transgenes were packaged into AAV capsids (mixed serotype 1 & 2, 1:1 ratio of AAV1 and AAV2 capsid proteins with AAV2 ITRs)^{44,47}. HEK293 cells were co-transfected, using the calcium phosphate method, with AAV transgene plasmid, the adenovirus helper plasmid *pF 6*, and the AAV helper plasmids *pH21* (AAV1), and *pRV1* (AAV2)⁴⁷. 60–65 hours after transfection, cells were washed in 1×PBS, and pelleted; pellets were resuspended in 150 mM NaCl, 20 mM Tris pH 8.0. Then sodium deoxycholate (Sigma #D5670) and benzonase endonuclease (Sigma #E1014) were added and incubated at 37 °C for 1 hr. After incubating, cell debris were removed by centrifugation and AAV particles were purified from the supernatant by passing over a heparin column (1-ml HiTrap Heparin columns, Sigma #5-4836), which binds the AAV particles⁴⁷. The column was pre-equilibrated with 10 ml 150 mM NaCl, 20 mM Tris pH 8.0. Then the supernatant was loaded onto the column at 200 µl/min flow rate; the column was washed with 20 ml 100 mM NaCl, 20 mM Tris pH 8.0 and virus was eluted off the column as follows: 1 ml 200 mM NaCl, 20 mM Tris pH 8.0 (discarded), 1 ml 300 mM NaCl, 20 mM Tris pH 8.0 (discarded), 1.5 ml 400 mM NaCl, 20 mM Tris pH 8.0 (collected), 3 ml 450 mM NaCl, 20 mM Tris pH 8.0 (collected), 1.5 ml 500 mM NaCl, 20 mM Tris pH 8.0 (collected). After purification, AAV particles were concentrated using AMICON ULTRA-4 (100000MWCO; Millipore; CatNo. UFC810024) at 2000g for 10 min. The concentrator was twice refilled with 3.5 ml of 0.9% NaCl. Elutions were removed to a sterile tube, and 250 µl of 0.9% NaCl were added. AAV was aliquotted and stored at –80 °C.

Mice

All experiments were performed in accordance with the United Kingdom Home Office Animal Procedures Act (1986), and had local ethical approval. All the knockdown and TetTag-DREADD experiments used adult male C57BL/6 mice, 8–12 weeks old, purchased from Harlan UK. The *vgat^{lox/lox}* mice³³ were purchased from JAX labs (stock NO. 012897; donated by Bradley Lowell). Mice were kept on a 12:12 light:dark cycle, at a maximum of four animals per cage, with free access to food and water. Behavioral experiments, except where specified otherwise, were performed during “lights-off”.

Stereotaxic injections of AAV

Mice were anesthetized with 2% isoflurane in O₂ by inhalation and mounted into a stereotaxic frame (Angle two, Leica Microsystems) linked to a digital mouse brain atlas. Mice were maintained on 1.5–2% isoflurane during the surgery. Mice that had been injected with AAVs were allowed 1 month to recover and for the viral transgenes to adequately express before undergoing behavioral experiments.

LC injections of *shadra2a1* and *shadra2a2* and shscramble AAVs

The AAVs to target the LC were injected into separate cohorts of adult C57BL/6 mice using 0.5 – 1 µl of virus, plus 0.5 µl 20% mannitol to increase injection spread⁴⁸, at 0.1 µl/min

controlled by an ultramicropump (World Precision Instruments), using pre-calibrated pulled glass pipettes with a tip diameter of 6 – 10 μm . Coordinates, measured in millimeter from Bregma were: -5.4 AP, ± 0.8 ML, -3.7 DV.

Preoptic hypothalamic injections of TetTag-DREADD and Cre-2A-Venus AAVs

The two TetTag-DREADD AAVs (AAV-*P_{cfos}-tTA* and AAV-*P_{TRE-tight-hM₃D_q-mCHERRY}*) were premixed in an equal ratio. AAV injections were done into adult C57BL/6 mice, with 0.5 μl of AAV mixture plus 0.5 μl 20% mannitol (total 1 μl volume). All injections used a 10 μl Hamilton syringe at a rate of 0.25 $\mu\text{l}/\text{min}$. The AAV-*Cre-2A-Venus* transgene⁴⁵ (gift from T. Kuner) was packaged into AAV capsids (see section, “Generation of Recombinant AAV particles”) and 0.5 μl AAV and 0.5 μl mannitol (20%) injected into adult *vgat^{lox/lox}* mice. AAVs were injected bilaterally into the LPO (AP +0.2 mm, ML ± 0.75 mm, DV -5.7 mm relative to Bregma), or with one injection into MnPO (AP +0.4 mm, ML 0 mm, DV -4.5 mm relative to Bregma), or bilateral injections into the superior colliculi (AP -3.8 mm, ML ± 1.0 mm, DV -2.0 mm relative to Bregma).

Fitting of Neurologgers

Mice were chronically implanted with skull screw electrodes (-1.5 mm Bregma, $+1.5$ mm midline – first recording electrode; $+1.5$ mm Bregma, -1.5 mm midline – second recording electrode; -1 mm Lambda, 0 mm midline – reference electrode) to measure cortical EEG and the electrical signals were recorded on a wireless electronic recording device (Neurologger 2) as described previously^{43,49}.

Assay for sedation

50 to 100 $\mu\text{g}/\text{kg}$ of dexmedetomidine (Tocris Bioscience, UK), dissolved in saline was delivered intraperitoneally and animals, fitted with Neurologgers, were placed immediately afterwards in the activity cage for 15 minutes to assess locomotor activity (Med Associates Activity Monitor Version 5 for mice). The EEG of animals was simultaneously recorded.

Assay for LORR

400 $\mu\text{g}/\text{kg}$ of dexmedetomidine was delivered intraperitoneally and animals, fitted with Neurologgers, were placed in a continuously slowly rotating cylinder⁴³. A rotation rate of 3 rpm was found to give a robust and reproducible LORR in control mice⁴³. Animals were scored as positive for LORR if they had rolled onto their backs in the rotating cylinder and made no obvious attempt to right themselves for at least 60 seconds. The EEG of animals was simultaneously recorded.

TetTag-pharmacogenetic behavioral protocols

After AAV injection, mice were raised on food with 40 mg/kg doxycycline (Harlan TD 120240 40 ppm Doxycycline Diet 2018B) for four weeks²⁴. For the behavioral experiments to examine dexmedetomidine-induced sedation, dexmedetomidine or saline *i.p.* injection took place 48 hours after removal of doxycycline. We chose this time point because it gave the optimum ratio of basal vs. induced transgene expression. At the end of the sedation experiments, mice were then put back on the doxycycline diet (Harlan TD 09295 1000 ppm

Doxycycline Diet 2018). Four days after dexmedetomidine-induced sedation, clozapine-N-oxide (C0832, Sigma-Aldrich, dissolved in saline, 5 mg/kg) was injected *i.p.* into TetTag-DREADD mice fitted with Neurologger2 devices. All CNO and dexmedetomidine injections were carried out during “lights off”. Thirty minutes after CNO injection, behavior was assessed in the activity cage as described under “Assay for sedation” (see above).

Sleep deprivation and recovery sleep

Sleep deprivation started 2 days after removal of doxycycline and started at Zeitgeber time zero. The control group was allowed normal sleep; the experimental group was sleep deprived for 4 hours by introducing novel objects or tapping lightly on the cages⁵⁰. To reduce the possibility of stress, we never touched the mice directly. Mice were then placed back into their home cages where they exhibited strong and sustained recovery NREM sleep. CNO (5 mg/kg) responses were examined four days from the recovery. At the end of the sleep recovery day, mice were put back on food with 1 g/kg doxycycline (or 1 g/l doxycycline in the drinking water), which was replaced with 40 mg/kg doxycycline the following day²⁴.

EEG analysis

Four data channels could be recorded at a sampling rate of 200 Hz and were low-pass filtered with a cut-off at 1 Hz (−3 db). The EEG data recorded by the Neurologger2 devices were downloaded and waveforms visualized using Spike2 software (Cambridge Electronic Design, Cambridge, UK) or MATLAB (MathWorks, Cambridge, UK). EEG data were analyzed using Fourier transforms to average power spectra over time⁴³. The power spectra were normalized such that the total area under the spectra for the saline controls was unity.

Measurement of body temperature

The body temperature of the mice was recorded using a miniature data logger (DSTnano; Star-Oddi, Gardabaer, Iceland) that was implanted seven days previously in the peritoneal cavity. The loggers were programmed to record every 30 minutes during 24-hour sleep recordings, every 5 minutes during sleep deprivation and recovery sleep, or every 2 minutes for experiments with dexmedetomidine or CNO injection. The loggers were recovered and the data downloaded at the end of the experiments.

Adra2a mRNA levels

Locus coeruleus *adra2a* mRNA levels were determined from *adra2a* KD and scramble AAV-injected mice by real time (quantitative, q)-PCR ($n=4$), using a Taqman® RNA-to-CTTM1-Step kit (Applied Biosystems, Foster City, USA). Briefly, brains were removed and 1-mm tissue punches were collected using 1-mm interval mouse brain matrix (Zivic Instruments, Pittsburgh, PA, USA) and 1-mm core diameter hollow needles. Total RNA was extracted from frozen tissues using TRIzol. qPCR was performed on an ABI StepOne Plus Real Time PCR system (Applied Biosystems, Foster City, USA) using the *adra2a* primers (Applied Biosystems, Mm00845983_s1, described previously⁴³). Data were evaluated with SDS 2.1 software, using the Comparative CT method (CT) to measure gene expression. Relative expression of the *adra2a* mRNA was determined by comparing AAV-shRNA mRNA levels

in the knockdown group to those in AAV-scramble, mice and normalized to expression of tyrosine hydroxylase (TH) mRNA (TH primers were: Applied Biosystems, Mm00447557_m1).

Immunohistochemistry (fluorescent detection)

Adult mice were anesthetized, transcardially perfused with 4% paraformaldehyde in PBS, pH 7.4. Brains were removed and 40- μ m-thick coronal sections cut using a Leica VT1000S vibratome. Free-floating sections were washed in PBS three times for 10 minutes, permeabilized in PBS plus 0.4% Triton X-100 for 30 min, blocked by incubation in PBS plus 4% normal goat serum (NGS), 0.2% Triton X-100 for 1 h (all at room temperature) and subsequently incubated with a cFOS monoclonal antibody²⁹ (1:10,000, Santa Cruz Biotechnology, CatNo.sc-253), and/or a *mCHERRY* monoclonal antibody (1:2000, Clontech CatNo.632543), or a tyrosine hydroxylase monoclonal antibody (1:1000, Sigma T-2928), or with GFP antiserum (1:1000, Life Technology, A6455)⁴⁴. Primary antisera were diluted in PBS plus 2% NGS overnight at 4°C. Incubated slices were washed three times in PBS plus 1% NGS for 10 minutes at room temperature, incubated for 2 h at room temperature with a 1:1000 dilution of a Alexa Fluor 488 goat anti-rabbit IgG (H+L) (1:1000, Molecular Probes®, CatNo.A11034) and Alexa Fluor® 594 goat anti-mouse IgG (H+L) (1:1000, Molecular Probes®, CatNo.A11005) in PBS plus 1% NGS, and subsequently washed three times in PBS for 10 min at room temperature. The sections were mounted on slides and coverslipped. Antibody validation: The cFOS antibody gave selective nuclear neuronal staining following an excitatory stimulus in a pattern consistent with many other studies (*e.g.* references 21 and 31) and staining with this antibody also mimicked the induction of the *cfos* promoter-based TetTag transgenes, further indicating specificity; the *mCHERRY* monoclonal antibody did not stain brain sections unless the area had been transduced with an AAV expressing the hM₃D_q-mCHERRY fusion protein; the tyrosine hydroxylase monoclonal antibody selectively stained neurons in the locus ceruleus, consistent with the known restricted expression of the tyrosine hydroxylase gene.

Immunohistochemistry (diaminobenzidine staining)

We used DAB staining to better visualize nuclear *cfos* expression over a relatively large area. 30 minutes after *i.p.* dexmedetomidine (50, 100, 400 μ g/kg), or saline (0.9%) administration, experimental mice were anesthetized, perfused transcardially, and free-floating sections processed for immunohistochemistry with rabbit antibody to Fos²⁹ (1:20,000, Ab-5, Calbiochem) after blocking endogenous peroxidase with 0.3% H₂O₂ in PBS. The primary antiserum was localized using a variation of the avidin-biotin complex system (Vector Laboratories). In brief, sections were incubated for 120 minutes at 22–25 °C in a solution of biotinylated goat antibody to rabbit IgG (PK-6101, Vector Laboratories) and then placed in the mixed avidin-biotin horseradish peroxidase complex solution (ABC Elite Kit, Vector Laboratories) for 60 minutes. The peroxidase complex was visualized by a 4 to 5-minute exposure to chromogen solution (0.05% 3,3'-diaminobenzidine tetrahydrochloride (wt/vol, Sigma-Aldrich), 0.4 mg/ml nickel ammonium sulfate to produce a blue-black product. The reaction was stopped by washing in distilled water and PBS. Sections were dehydrated and cover-slipped with quick mounting medium (Eukitt, Fluka Analytical).

Electrophysiology and single-cell qPCR

For acute brain slice recordings of LPO and LC neurons, 250 μ m-sections were cut with a Vibratome (Campden Instruments) in ice-cold slicing solution containing (in mM): 85 NaCl, 2.5 KCl, 1 CaCl₂, 4 MgCl₂, 1.25 NaH₂PO₄, 26 NaHCO₃, 75 sucrose, 25 glucose, pH 7.4 when bubbled with 95% O₂ and 5% CO₂. After incubating in slicing solution for 15–30 minutes at room temperature, slices were then transferred to oxygenated ACSF containing (in mM): NaCl 125, KCl 2.5, CaCl₂ 2, MgCl₂ 1, NaH₂PO₄ 1.25, NaHCO₃ 26, glucose 11. For the LC recordings, the solution also contained 1 mM kynurenic acid. For whole-cell current clamp recordings, patch pipettes (4–6 M Ω) were backfilled with internal solution containing (in mM): 145 K-gluconate, 4 NaCl, 5 KCl, 0.5 CaCl₂, 5 EGTA, 10 HEPES, 4 Mg-ATP, 0.3 Na-GTP, and 10 sucrose, pH 7.3, adjusted with KOH for the LPO recordings and (in mM) 130 KCl, 10 HEPES, 0.1 BAPTA, 5 MgCl₂, 3 Na₂-ATP, 0.1 Na-GTP, 8 phosphocreatine, pH 7.3 for the LC recordings²⁹.

For single-cell qPCR, after achieving a whole-cell recording the content of the neuron was aspirated under visual control into the recording pipette and expelled into single cell lysis/DNAseI solution using the Single-Cell-to-CT Kit (Ambion). Reverse transcription, cDNA pre-amplification and qPCR were performed following the manufacturer's guidelines using the TaqMan® Gene Expression Assay system (Applied Biosystems, Foster City, USA). The primer reference numbers were: *hprt*: Mm01545399_m1; *gad1*: Mm00725661_s1; *gad2*: Mm00484623_m1; *vglut1*: Mm00812886_m1; *vglut2*: Mm00499876_m1.

Statistical analyses

Prism6 and Origin were used for statistical analysis. No statistical methods were used to predetermine sample sizes, but our sample sizes are similar to those reported in previous publications (16, 29 & 31). Data collection and processing were randomized or performed in a counter-balanced manner. Normality was tested by the Shapiro-Wilk test. Equal variances were assessed by F-test. Data are represented as the mean \pm s.e.m. For qPCR, LORR and cFOS immunohistochemistry, Fisher's exact test or a two-tailed unpaired t test was performed. For the dexmedetomidine sedation and DREADD behavioral experiments, two-way ANOVA was performed. $P < 0.05$ was considered significant (* $P < 0.05$, ** $P < 0.01$, *** $P < 0.001$). Mice were excluded from the analysis if the histology did not confirm significant mCHERRY expression in LPO or MnPO, or if the EEG/EMG recording technology failed during the experiment. In the *adra2a* knockdown experiments (Fig. 1) and *vgat* deletion experiments (Fig. 7), mice brains that had undetectable AAV transgene expression, or with expression beyond the target region, were excluded from the statistics. All the experiments were performed and analyzed blind to treatment conditions.

Supplementary Material

Refer to Web version on PubMed Central for supplementary material.

Acknowledgments

This work was supported by the Medical Research Council, UK (G0901892, N.P.F. and W.W.; G0800399, W.W.), the BBSRC (G021691 and BB/K018159/1, N.P.F. and W.W.), a BBSRC CASE studentship (E.A.S.), a Wellcome

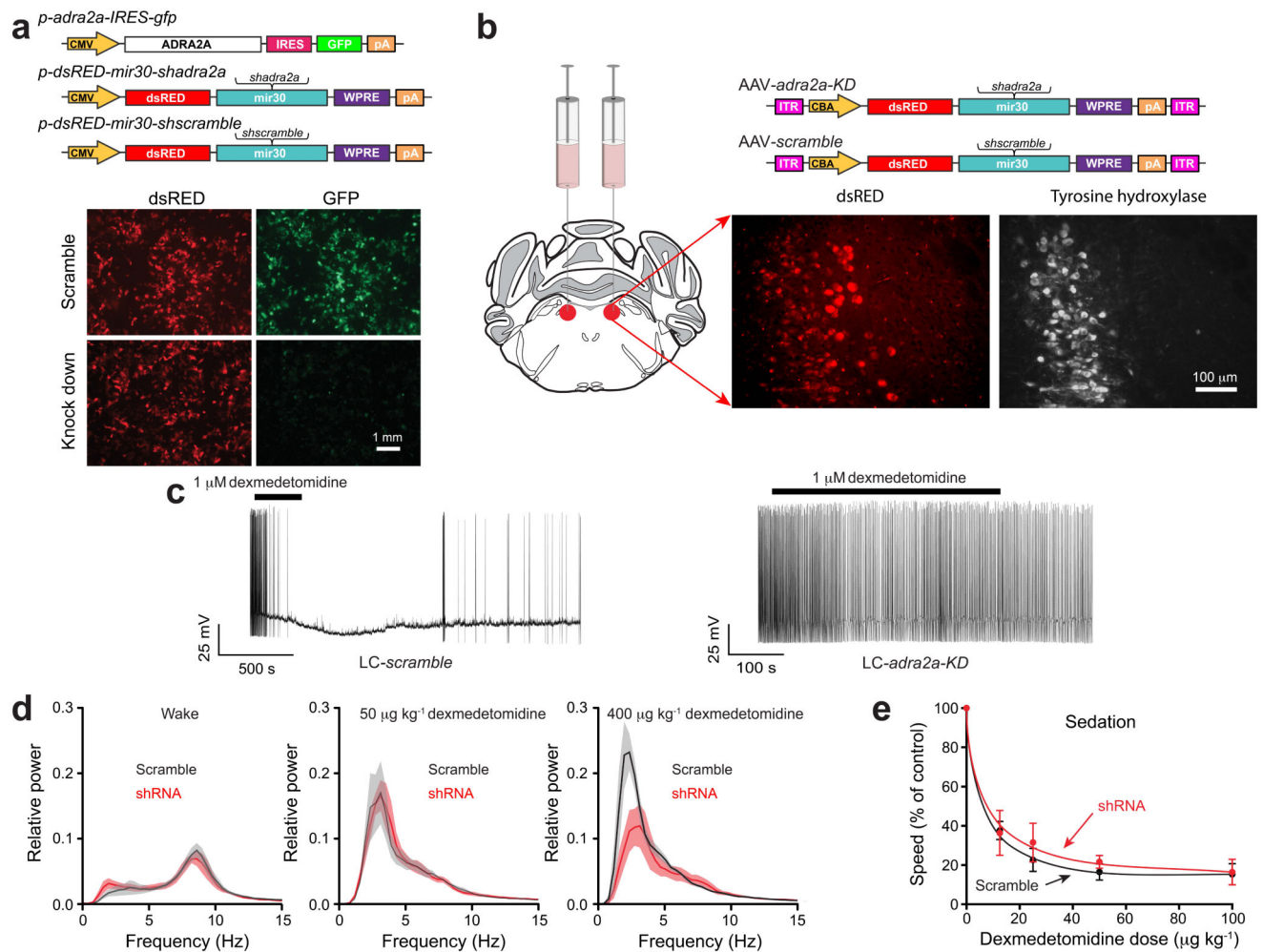
Trust Vacation Scholarship (Z.E.P.), a BBSRC doctoral training grant (BB/F017324/1) (E.C.H), UK-China Scholarships for Excellence/China Scholarship scheme (X.Y. and Z.Y.) and the ERASMUS program (I.G. & A.M.)

References

1. Franks NP. General anaesthesia: from molecular targets to neuronal pathways of sleep and arousal. *Nature reviews. Neuroscience.* 2008; 9:370–386. [PubMed: 18425091]
2. Rihel J, Schier AF. Sites of action of sleep and wake drugs: insights from model organisms. *Current opinion in neurobiology.* 2013; 23:831–840. [PubMed: 23706898]
3. Adams R, et al. Efficacy of dexmedetomidine compared with midazolam for sedation in adult intensive care patients: a systematic review. *British journal of anaesthesia.* 2013; 111:703–710. [PubMed: 23748199]
4. Bol C, Danhof M, Stanski DR, Mandema JW. Pharmacokinetic-pharmacodynamic characterization of the cardiovascular, hypnotic, EEG and ventilatory responses to dexmedetomidine in the rat. *The Journal of pharmacology and experimental therapeutics.* 1997; 283:1051–1058. [PubMed: 9399976]
5. Seidel WF, Maze M, Dement WC, Edgar DM. Alpha-2 adrenergic modulation of sleep: time-of-day-dependent pharmacodynamic profiles of dexmedetomidine and clonidine in the rat. *The Journal of pharmacology and experimental therapeutics.* 1995; 275:263–273. [PubMed: 7562559]
6. MacDonald E, Scheinin M, Scheinin H, Virtanen R. Comparison of the behavioral and neurochemical effects of the two optical enantiomers of medetomidine, a selective alpha-2-adrenoceptor agonist. *The Journal of pharmacology and experimental therapeutics.* 1991; 259:848–854. [PubMed: 1682487]
7. Sanders RD, Maze M. Noradrenergic trespass in anesthetic and sedative states. *Anesthesiology.* 117:945–947. [PubMed: 23042229]
8. Nelson LE, et al. The alpha2-adrenoceptor agonist dexmedetomidine converges on an endogenous sleep-promoting pathway to exert its sedative effects. *Anesthesiology.* 2003; 98:428–436. [PubMed: 12552203]
9. Lakhani PP, et al. Substitution of a mutant alpha2a-adrenergic receptor via “hit and run” gene targeting reveals the role of this subtype in sedative, analgesic, and anesthetic-sparing responses in vivo. *Proceedings of the National Academy of Sciences of the United States of America.* 1997; 94:9950–9955. [PubMed: 9275232]
10. Aghajanian GK, VanderMaelen CP. alpha 2-adrenoceptor-mediated hyperpolarization of locus coeruleus neurons: intracellular studies in vivo. *Science.* 1982; 215:1394–1396. [PubMed: 6278591]
11. Correa-Sales C, Rabin BC, Maze M. A hypnotic response to dexmedetomidine, an alpha 2 agonist, is mediated in the locus coeruleus in rats. *Anesthesiology.* 1992; 76:948–952. [PubMed: 1350889]
12. Takahashi K, Kayama Y, Lin JS, Sakai K. Locus coeruleus neuronal activity during the sleep-waking cycle in mice. *Neuroscience.* 2010; 169:1115–1126. [PubMed: 20542093]
13. Berridge CW, Schmeichel BE, Espana RA. Noradrenergic modulation of wakefulness/arousal. *Sleep medicine reviews.* 2012; 16:187–197. [PubMed: 22296742]
14. Carter ME, de Lecea L, Adamantidis A. Functional wiring of hypocretin and LC-NE neurons: implications for arousal. *Frontiers in behavioral neuroscience.* 2013; 7:43. [PubMed: 23730276]
15. Carter ME, et al. Tuning arousal with optogenetic modulation of locus coeruleus neurons. *Nature neuroscience.* 2010; 13:1526–1533. [PubMed: 21037585]
16. Gilsbach R, et al. Genetic dissection of alpha2-adrenoceptor functions in adrenergic versus nonadrenergic cells. *Molecular pharmacology.* 2009; 75:1160–1170. [PubMed: 19251826]
17. Hu FY, et al. Hypnotic hypersensitivity to volatile anesthetics and dexmedetomidine in dopamine beta-hydroxylase knockout mice. *Anesthesiology.* 2012; 117:1006–1017. [PubMed: 23042227]
18. Szymusiak R, Gvilia I, McGinty D. Hypothalamic control of sleep. *Sleep medicine.* 2007; 8:291–301. [PubMed: 17468047]
19. Alam MA, Kumar S, McGinty D, Alam MN, Szymusiak R. Neuronal activity in the preoptic hypothalamus during sleep deprivation and recovery sleep. *Journal of neurophysiology.* 2014; 111:287–299. [PubMed: 24174649]

20. Takahashi K, Lin JS, Sakai K. Characterization and mapping of sleep-waking specific neurons in the basal forebrain and preoptic hypothalamus in mice. *Neuroscience*. 2009; 161:269–292. [PubMed: 19285545]
21. Sherin JE, Shiromani PJ, McCarley RW, Saper CB. Activation of ventrolateral preoptic neurons during sleep. *Science*. 1996; 271:216–219. [PubMed: 8539624]
22. Lu J, Greco MA, Shiromani P, Saper CB. Effect of lesions of the ventrolateral preoptic nucleus on NREM and REM sleep. *The Journal of neuroscience: the official journal of the Society for Neuroscience*. 2000; 20:3830–3842. [PubMed: 10804223]
23. Saper CB, Fuller PM, Pedersen NP, Lu J, Scammell TE. Sleep state switching. *Neuron*. 2010; 68:1023–1042. [PubMed: 21172606]
24. Reijmers LG, Perkins BL, Matsuo N, Mayford M. Localization of a stable neural correlate of associative memory. *Science*. 2007; 317:1230–1233. [PubMed: 17761885]
25. Garner AR, et al. Generation of a synthetic memory trace. *Science*. 2012; 335:1513–1516. [PubMed: 22442487]
26. Reijmers L, Mayford M. Genetic control of active neural circuits. *Frontiers in molecular neuroscience*. 2009; 2:27. [PubMed: 20057936]
27. Alexander GM, et al. Remote control of neuronal activity in transgenic mice expressing evolved G protein-coupled receptors. *Neuron*. 2009; 63:27–39. [PubMed: 19607790]
28. Stegmeier F, Hu G, Rickles RJ, Hannon GJ, Elledge SJ. A lentiviral microRNA-based system for single-copy polymerase II-regulated RNA interference in mammalian cells. *Proceedings of the National Academy of Sciences of the United States of America*. 2005; 102:13212–13217. [PubMed: 16141338]
29. Zecharia AY, et al. The involvement of hypothalamic sleep pathways in general anesthesia: testing the hypothesis using the GABA_A receptor beta3N265M knock-in mouse. *The Journal of neuroscience: the official journal of the Society for Neuroscience*. 2009; 29:2177–2187. [PubMed: 19228970]
30. Tan CM, Wilson MH, MacMillan LB, Kobilka BK, Limbird LE. Heterozygous alpha 2A-adrenergic receptor mice unveil unique therapeutic benefits of partial agonists. *Proceedings of the National Academy of Sciences of the United States of America*. 2002; 99:12471–12476. [PubMed: 12205290]
31. Gong H, et al. Activation of c-fos in GABAergic neurones in the preoptic area during sleep and in response to sleep deprivation. *The Journal of physiology*. 2004; 556:935–946. [PubMed: 14966298]
32. Hunter JC, et al. Assessment of the role of alpha2-adrenoceptor subtypes in the antinociceptive, sedative and hypothermic action of dexmedetomidine in transgenic mice. *British journal of pharmacology*. 1997; 122:1339–1344. [PubMed: 9421280]
33. Tong Q, Ye CP, Jones JE, Elmquist JK, Lowell BB. Synaptic release of GABA by AgRP neurons is required for normal regulation of energy balance. *Nature neuroscience*. 2008; 11:998–1000. [PubMed: 19160495]
34. Drew GM, Gower AJ, Marriott AS. Alpha 2-adrenoceptors mediate clonidine-induced sedation in the rat. *British journal of pharmacology*. 1979; 67:133–141. [PubMed: 40643]
35. McGregor R, Siegel JM. Illuminating the locus coeruleus: control of posture and arousal. *Nature neuroscience*. 2010; 13:1448–1449. [PubMed: 21102568]
36. McGinty DJ, Serman MB. Sleep suppression after basal forebrain lesions in the cat. *Science*. 1968; 160:1253–1255. [PubMed: 5689683]
37. Serman MB, Clemente CD. Forebrain inhibitory mechanisms: sleep patterns induced by basal forebrain stimulation in the behaving cat. *Experimental neurology*. 1962; 6:103–117. [PubMed: 13916976]
38. Sherin JE, Elmquist JK, Torrealba F, Saper CB. Innervation of histaminergic tuberomammillary neurons by GABAergic and galaninergic neurons in the ventrolateral preoptic nucleus of the rat. *The Journal of neuroscience: the official journal of the Society for Neuroscience*. 1998; 18:4705–4721. [PubMed: 9614245]
39. Saito YC, et al. GABAergic neurons in the preoptic area send direct inhibitory projections to orexin neurons. *Frontiers in neural circuits*. 2013; 7:192. [PubMed: 24348342]

40. Gallopin T, et al. Identification of sleep-promoting neurons in vitro. *Nature*. 2000; 404:992–995. [PubMed: 10801127]
41. Modirrousta M, Mainville L, Jones BE. Gabaergic neurons with alpha2-adrenergic receptors in basal forebrain and preoptic area express c-Fos during sleep. *Neuroscience*. 2004; 129:803–810. [PubMed: 15541901]
42. Brown RE, Basheer R, McKenna JT, Strecker RE, McCarley RW. Control of sleep and wakefulness. *Physiological reviews*. 2012; 92:1087–1187. [PubMed: 22811426]
43. Gelegen C, et al. Staying awake – a genetic region that hinders alpha adrenergic receptor agonist-induced sleep. *The European journal of neuroscience*. 2014
44. Murray AJ, et al. Parvalbumin-positive CA1 interneurons are required for spatial working but not for reference memory. *Nature neuroscience*. 2011; 14:297–299. [PubMed: 21278730]
45. Tang W, et al. Faithful expression of multiple proteins via 2A-peptide self-processing: a versatile and reliable method for manipulating brain circuits. *The Journal of neuroscience: the official journal of the Society for Neuroscience*. 2009; 29:8621–8629. [PubMed: 19587267]
46. Krashes MJ, et al. Rapid, reversible activation of AgRP neurons drives feeding behavior in mice. *The Journal of clinical investigation*. 2011; 121:1424–1428. [PubMed: 21364278]
47. Klugmann M, et al. AAV-mediated hippocampal expression of short and long Homer 1 proteins differentially affect cognition and seizure activity in adult rats. *Molecular and cellular neurosciences*. 2005; 28:347–360. [PubMed: 15691715]
48. Mastakov MY, Baer K, Xu R, Fitzsimons H, During MJ. Combined injection of rAAV with mannitol enhances gene expression in the rat brain. *Molecular therapy: the journal of the American Society of Gene Therapy*. 2001; 3:225–232. [PubMed: 11237679]
49. Vyssotski AL, et al. EEG responses to visual landmarks in flying pigeons. *Current biology: CB*. 2009; 19:1159–1166. [PubMed: 19559612]
50. Gerashchenko D, et al. Identification of a population of sleep-active cerebral cortex neurons. *Proceedings of the National Academy of Sciences of the United States of America*. 2008; 105:10227–10232. [PubMed: 18645184]

**Figure 1.**

Knock down of adrenergic α 2A receptors in the locus coeruleus blocks dexmedetomidine-induced LORR, but not sedation. **(a)** Testing shRNAs for knockdown efficacy of *adra2a-IRES-gfp* transgene expression in HEK-293 cells ($n=8$). The photographs show transfected HEK-293 cells; GFP fluorescence (green) was strongly reduced with the *shadra2a*₁ construct but not with the scramble version. The dsRED expression reveals similar transfection efficiencies. CMV, cytomegalovirus promoter/enhancer region; IRES, internal ribosome entry site; pA, polyadenylation sequence; WPRE, woodchuck post-transcriptional regulatory element. **(b)** AAVs expressing either *dsRED-mir30-shadra2a* or *dsRED-mir30-shscramble* transgenes were bilaterally injected into the LC of adult mice. Photographs illustrate AAV transgene expression (dsRED) in the LC as confirmed by co-staining with tyrosine hydroxylase antisera (white). ITR, inverted terminal repeats; CBA, chicken- β -actin enhancer/promoter. **(c)** Whole-cell recordings of action potentials of LC neurons, in acute slices from LC-*scramble*, and LC-*adra2a-KD* mice. Applying dexmedetomidine to scramble-expressing neurons hyperpolarized the membrane potential and the neurons stopped firing; by contrast dexmedetomidine had no effect on the neurons from the LC-*adra2a-KD* mice ($P=0.7$; $n=7$ cells). **(d)** Fourier transform power spectra for LC-*scramble*

(black), and LC-*adra2a-KD* (red) mice in the waking state (left; $n=5$) and in response to 50 $\mu\text{g kg}^{-1}$ dexmedetomidine (middle; $n=4$) and 400 $\mu\text{g kg}^{-1}$ dexmedetomidine (right; $n=4$). Lighter shaded envelopes indicate the s.e.m. (e) Movement of LC-*scramble* (black; $n=4-6$), and LC-*adra2a-KD* (red; $n=4-7$) mice in response to sedative doses of dexmedetomidine were not significantly different (two-way ANOVA, $P=0.91$).

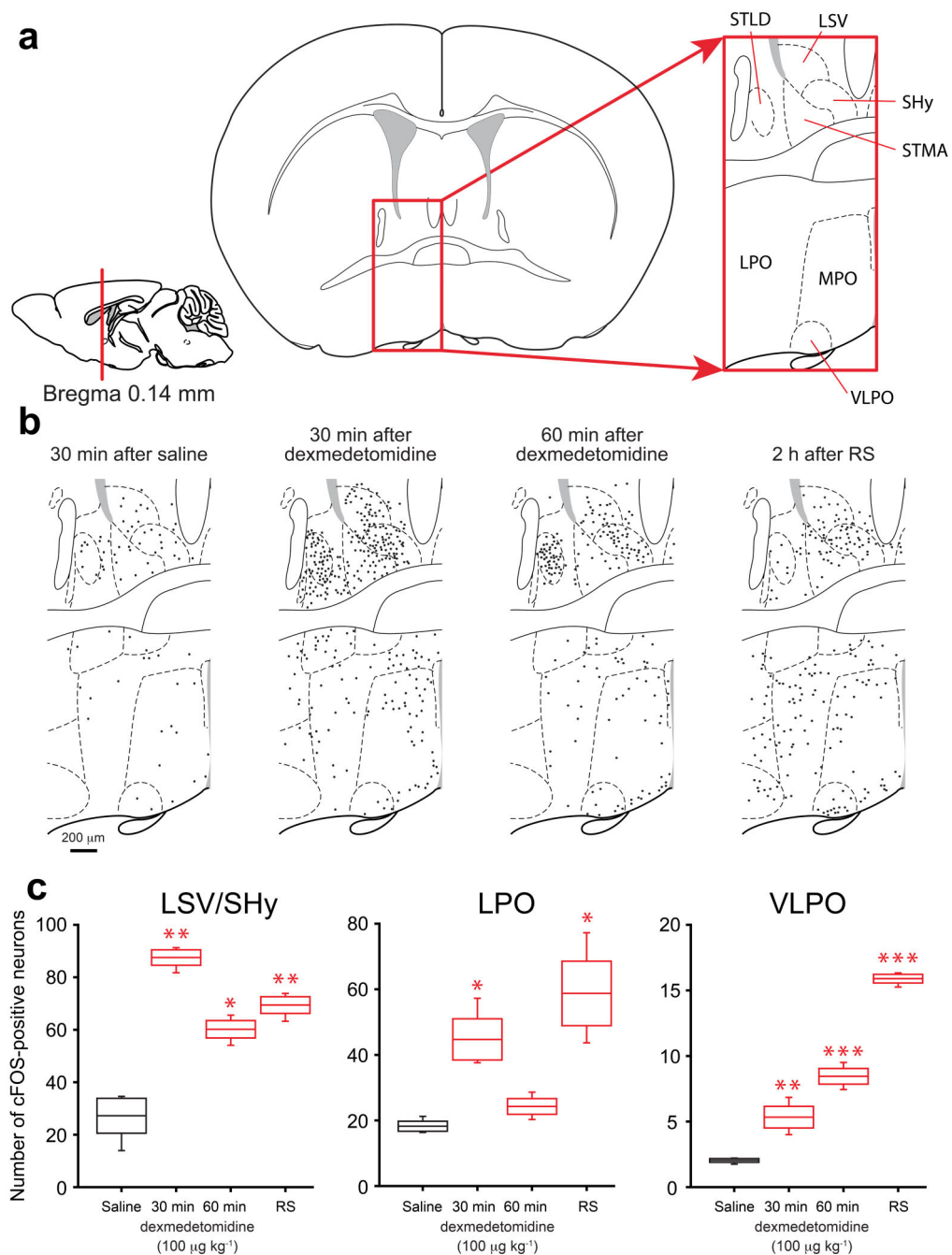


Figure 2.

Dexmedetomidine-induced sedation and recovery sleep induced cFOS expression in overlapping regions of the mouse hypothalamic preoptic area and septum. **(a)** Schematic of the relevant preoptic hypothalamic and septal areas: left-hand drawing, midline-sagittal section, red line marks position of the section; middle drawing, coronal section, boxed area, magnified on the right, shows the relevant anatomical sites. **(b)** Line drawings of cFOS protein expression in the boxed area at 30 minutes after saline injection and 30 or 60 minutes after dexmedetomidine (100 µg/kg) injections or 2 hours into recovery sleep after sleep

deprivation; black dots represent cFOS-positive cells (see Supplementary Fig. 1 for representative photographs); relative to its expression after a saline injection, the endogenous *cfos* gene is induced widely in the area by sedative doses of dexmedetomidine or during recovery sleep. (c) Number of cFOS positive neurons in selected anatomical sites after saline (white) or dexmedetomidine (red) injections or recovery sleep (gray). The boxes represent the s.e.m, and the bars show the range of the data. Asterisks represent significance relative to saline * $P < 0.05$, ** $P < 0.01$, *** $P < 0.001$ (t -test). LPO, lateral preoptic area; LSV, lateral septum, ventral; MPO, medial preoptic area SHy, septo-hypothalamic nucleus; STLD, stria terminalis lateral dorsal; STMA, stria terminalis medial anterior; VLPO, ventral lateral preoptic area.

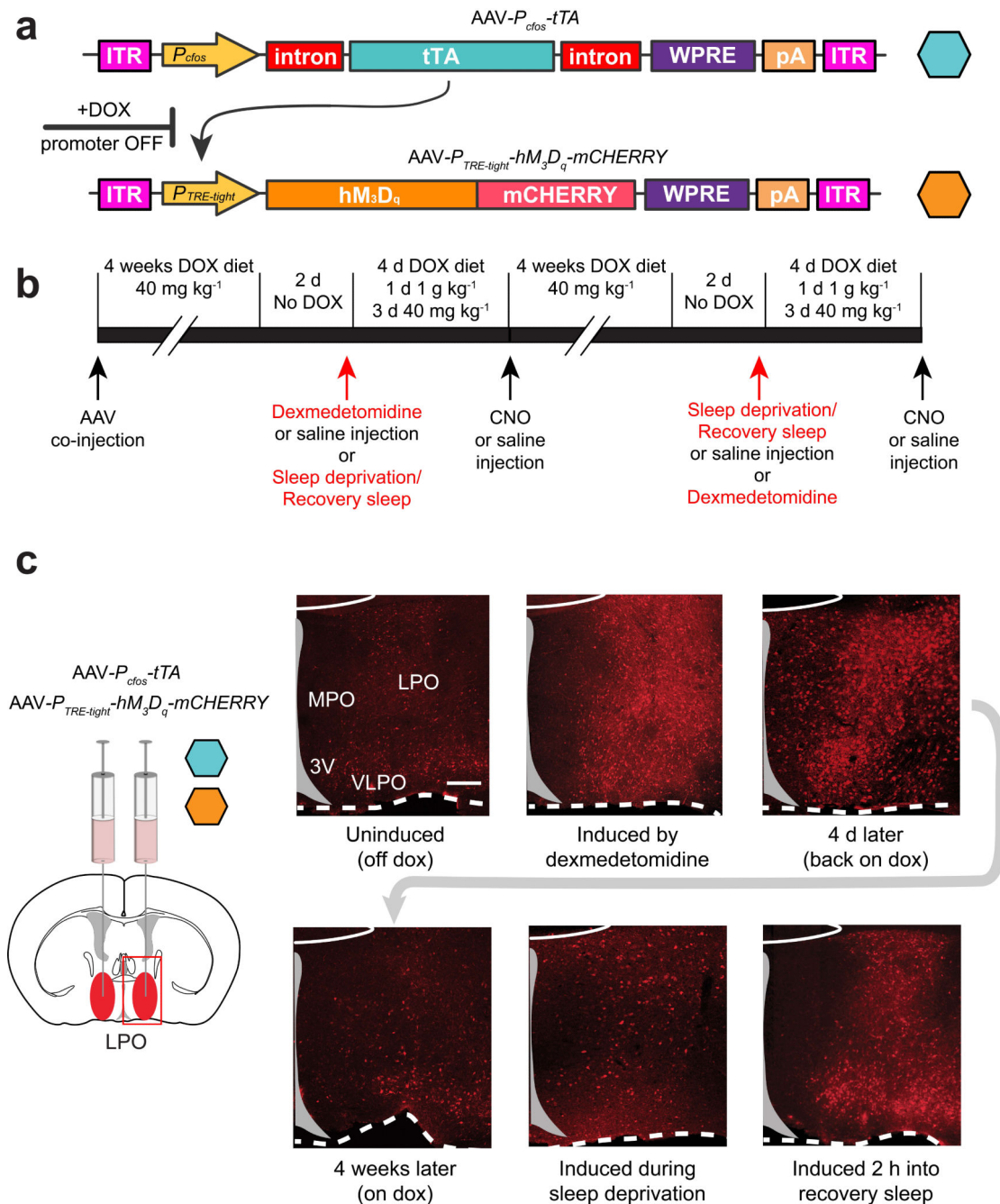


Figure 3.

The TetTag- hM_3D_q system to record and reactivate neuronal groups in the preoptic hypothalamus activated by a sedative dose of dexmedetomidine or during recovery sleep. **(a)** The AAV transgenes: the first contains the *cfos* promoter, which drives expression of tTA protein. In the presence of doxycycline (DOX), tTA cannot bind and activate its target promoter, $P_{TRE-tight}$ located in the second AAV genome; when doxycycline is removed, tTA can activate hM_3D_q -mCherry expression but only in neurons where tTA expression had been driven by the *cfos* promoter, reflecting neural activity. **(b)** The extended protocol and

time-line for the experiments. (c) LPO-*TetTag-hM₃D_q* mice. Time course of *P_{TRE-tight}-hM₃D_q-mCHERRY* transgene induction and decay. The photographs show coronal sections from one side of the brain stained for *hM₃D_q-mCHERRY* expression (red), detected with *mCHERRY* antisera. The images were taken from animals killed at six time points: with doxycycline removed from the diet two days previously, just before dexmedetomidine-induced sedation; 2 hours after a sedative dose of dexmedetomidine; 4 days later on and back on doxycycline, 4 weeks after dexmedetomidine-induced sedation on a doxycycline diet; 4 hours after sleep deprivation; and 2 hours into recovery sleep following sleep deprivation. Induced *hM₃D_q-mCHERRY* transgene expression was seen throughout the LPO area. Scale bar, 200 μ m.

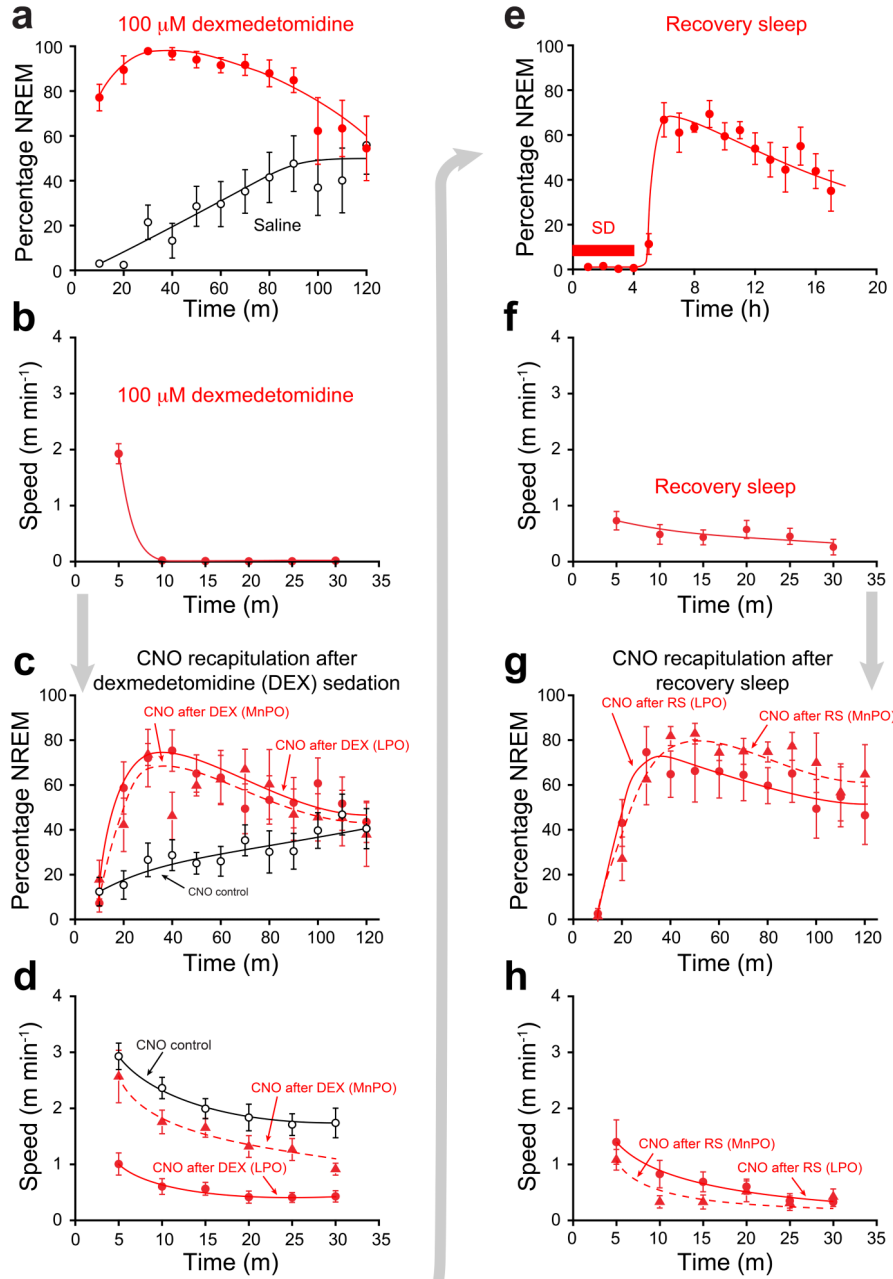


Figure 4. Serial re-activation of genetically tagged neuronal ensembles following dexmedetomidine-induced sedation and recovery sleep. (a) Percentage NREM sleep after dexmedetomidine. Both LPO- *TetTag-hM₃D_q* ($n=6$) and MnPO- *TetTag-hM₃D_q* ($n=6$) mice showed sustained NREM, significantly greater than control ($P<0.0001$). Data shown are for LPO- *TetTag-hM₃D_q* mice. (b) Speed in an open field 30 min after dexmedetomidine. Data shown are for LPO- *TetTag-hM₃D_q* mice ($n=7$). (c) NREM sleep after CNO injection, four days after dexmedetomidine sedation. Filled circles: LPO- *TetTag-hM₃D_q* mice ($n=7$; $P<0.0001$,

compared to control) after CNO injection. Filled triangles: MnPO-*TetTag-hM₃D_q* ($n=6$; $P<0.001$, compared to control) mice after CNO injection. Open circles: LPO-*TetTag-hM₃D_q* ($n=9$) mice after control CNO injection without prior sedation or recovery sleep. **(d)** Speed in an open field 30 min after CNO injection, four days after dexmedetomidine sedation. Filled circles: after CNO injection for LPO-*TetTag-hM₃D_q* mice. Filled triangles: after CNO injection for MnPO-*TetTag-hM₃D_q* mice. Open circles: after control CNO injection without prior sedation or recovery sleep. CNO recapitulated the effects of dexmedetomidine in LPO-*TetTag-hM₃D_q* ($n=8$; $P<0.0001$) but not in MnPO-*TetTag-hM₃D_q* mice ($n=6$; $P=0.1$) compared to control ($n=7$). **(e)** NREM after 4 hours sleep deprivation (SD) ($n=6$). **(f)** Speed in an open field 30 min during recovery sleep ($n=8$). **(g)** NREM sleep after CNO injection, four days after sleep deprivation/recovery sleep. Filled circles: LPO-*TetTag-hM₃D_q* mice ($n=8$; $P<0.0001$, compared to baseline) after CNO injection. Filled triangles: MnPO-*TetTag-hM₃D_q* ($n=7$; $P<0.0001$, two-way ANOVA compared to baseline) mice after CNO injection. **(h)** Speed in open field 30 min after CNO injection, four days after recovery sleep. CNO recapitulated the effects of recovery sleep in both LPO-*TetTag-hM₃D_q* ($n=8$; $P<0.0001$) and in MnPO-*TetTag-hM₃D_q* mice ($n=7$; $P<0.0001$, two-way ANOVA) compared to baseline ($n=7$). For all panels the error bars represent s.e.m and the statistical tests were two-way ANOVA.

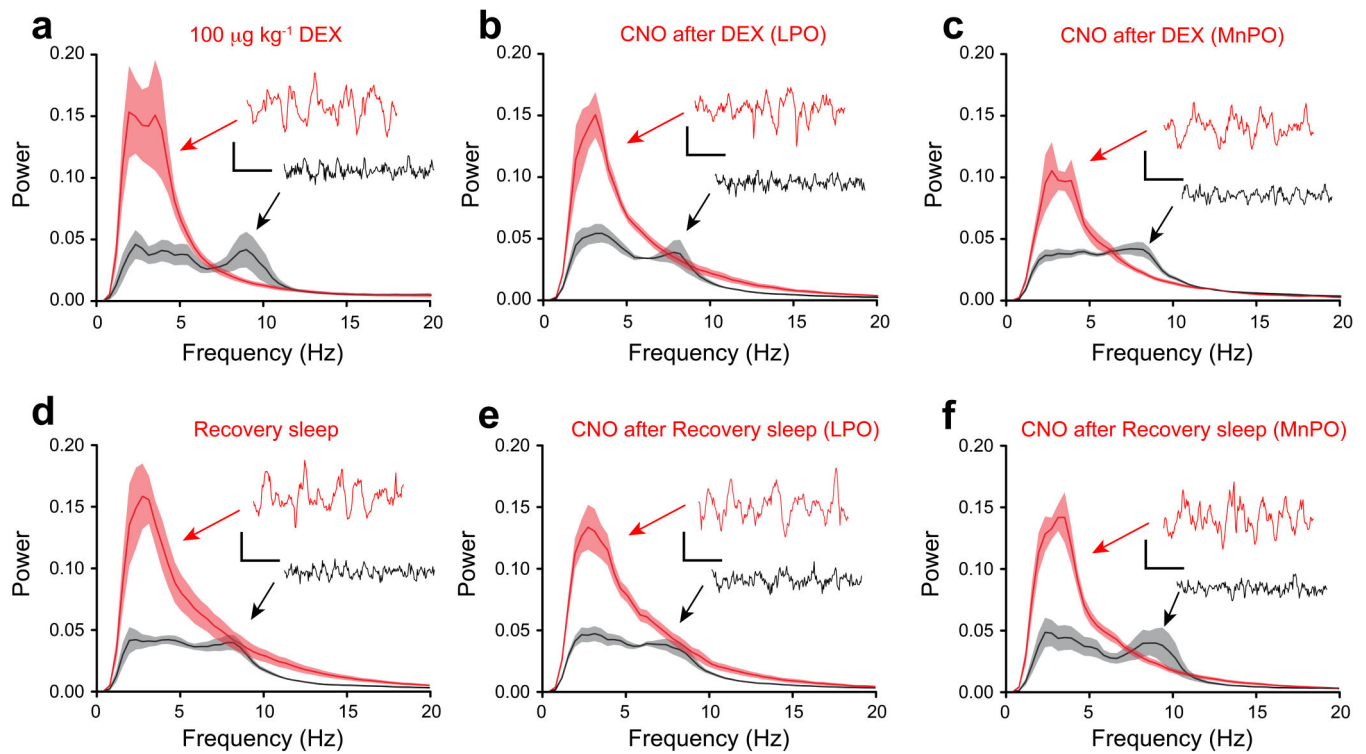


Figure 5.

EEG delta power is recapitulated by reactivation of genetically tagged neuronal ensembles in LPO-*TetTag-hM₃D_q* and MnPO-*TetTag-hM₃D_q* mice following dexmedetomidine-induced sedation or recovery sleep. Each panel shows Fourier Transform power spectra when the EEG and EMG signals were scored as either sleep (red) or wake (black). The envelopes represent the s.e.m. (a) Dexmedetomidine sedation ($n=7$). (b) CNO reactivation after dexmedetomidine sedation for LPO-*TetTag-hM₃D_q* mice ($n=8$). (c) CNO reactivation after dexmedetomidine sedation for MnPO-*TetTag-hM₃D_q* mice ($n=6$). (d) Recovery sleep ($n=7$). (e) CNO reactivation after recovery sleep for LPO-*TetTag-hM₃D_q* mice ($n=8$). (f) CNO reactivation after recovery sleep for MnPO-*TetTag-hM₃D_q* mice ($n=7$). Each spectrum is calculated by combining EEG segments totally 20 minutes. The inserts show representative EEG traces, and the accompanying calibration bars represent 100 μV and 500 msec.

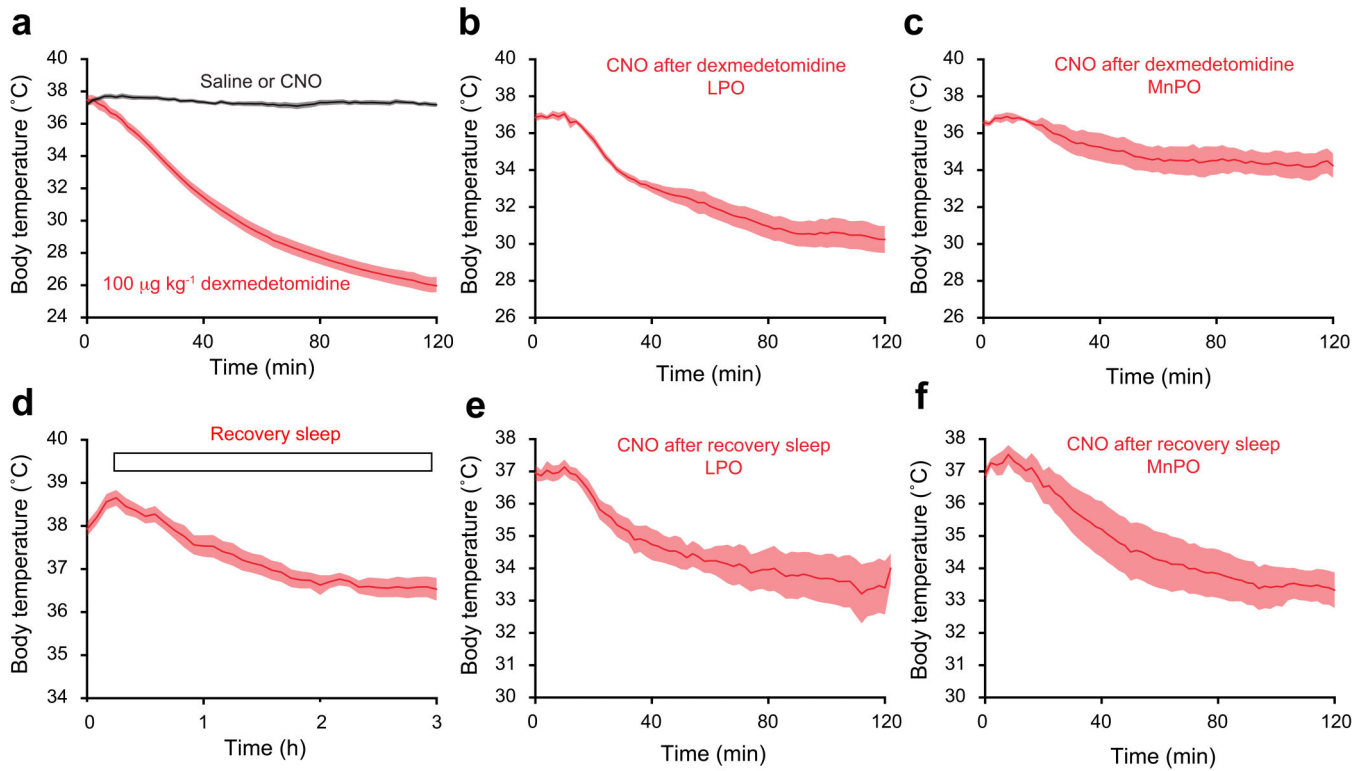


Figure 6.

Hypothermia is recapitulated by reactivation of genetically tagged neuronal ensembles in LPO-*TetTag-hM₃D_q* and MnPO-*TetTag-hM₃D_q* mice following recovery sleep, but only in LPO-*TetTag-hM₃D_q* mice following dexmedetomidine-induced sedation. Each panel shows changes in body temperature following: (a) dexmedetomidine sedation ($n=10$) (red) or saline ($n=20$) or CNO ($n=3$) (black), (b) CNO reactivation after dexmedetomidine sedation for LPO-*TetTag-hM₃D_q* mice ($n=5$), (c) CNO reactivation after dexmedetomidine sedation for MnPO-*TetTag-hM₃D_q* mice ($n=5$), (d) recovery sleep ($n=10$), (e) CNO reactivation after recovery sleep for LPO-*TetTag-hM₃D_q* mice ($n=6$), and (f) CNO reactivation after recovery sleep for MnPO-*TetTag-hM₃D_q* mice ($n=5$). The data in panels a) and d) are for LPO-*TetTag-hM₃D_q* and MnPO-*TetTag-hM₃D_q* mice combined, because these were indistinguishable.

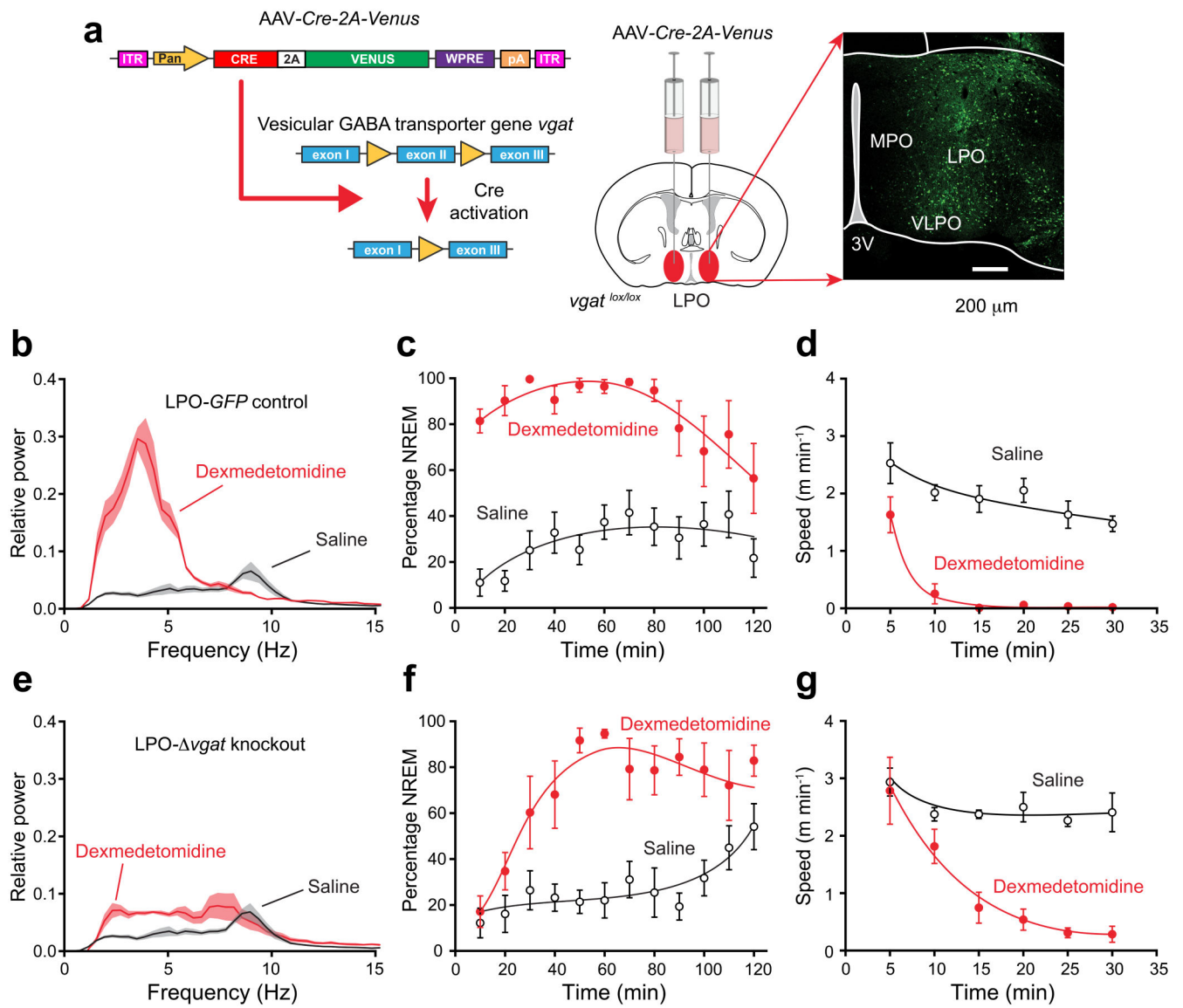


Figure 7. Selective knockout of the GABA vesicular transporter gene (*vgat*) in the PO hypothalamic area (LPO- *vgat* mice) slows the transition to dexmedetomidine-induced sleep. **(a)** Cre recombinase, produced from an AAV transgene, deletes exon 2 of the *vgat* gene³³ following AAV-*Cre-2A-Venus* bilateral injection into the LPO area of *vgat*^{lox/lox} mice. The image on the right shows the extent of AAV expression, as detected by staining with EGFP antisera. **(b)** EEG power spectra ten minutes after dexmedetomidine (100 μ g kg⁻¹ – red line) or saline (black) injection in control mice ($n=8$) expressing AAV-*GFP* in the LPO (LPO-*GFP* mice; $n=6$). Lighter shaded envelopes indicate the s.e.m. **(c)** Percentage of time scored as NREM sleep after dexmedetomidine (100 μ g/kg; filled circles, $n=6$) was significantly greater (two-way ANOVA, $P<0.0001$) than in saline (open circles, $n=8$) in LPO-*GFP* control mice. **(d)** Speed in open field 30 min after dexmedetomidine (100 μ g kg⁻¹; filled circles, $n=7$) was significantly less (two-way ANOVA, $P<0.0001$) than in saline (open circles, $n=6$) in LPO-

GFP control mice. (e) EEG power spectra ten minutes after dexmedetomidine (100 $\mu\text{g}/\text{kg}$ – red line; $n=6$) or saline (black) injection in mice ($n=8$) expressing AAV-*Cre-2A-Venus* in the LPO (LPO- *vgat* mice). (f) Percentage of time scored as NREM sleep after dexmedetomidine (100 $\mu\text{g}/\text{kg}$; filled circles, $n=6$) was significantly greater (two-way ANOVA, $P<0.0001$) than in saline ($n=8$) in AAV-*Cre-2A-Venus* mice. (g) Speed in open field 30 min after dexmedetomidine (100 $\mu\text{g}/\text{kg}$; filled circles, $n=6$) was significantly less (two-way ANOVA, $P<0.0001$) than in saline (open circles, $n=8$) in LPO- *vgat* mice. For all panels the error bars represent s.e.m.